Supplementary Information:

Linking hydrothermal deactivation of Cu-CHA catalysts for NH_3-SCR to dealumination and reduced $[Cu_2(NH_3)_4O_2]^{2+}$ formation

Shivangi Singh,[*,†,‡] Ton V. W. Janssens,[¶] and Henrik Grönbeck[*,‡]

†*Umicore Denmark ApS, DK-2970 Hørsholm, Denmark*

‡*Department of Physics and Competence Centre for Catalysis, Chalmers University of Technology, SE-412 96 Göteborg, Sweden*

¶*c/o Umicore AG & Co. KG, Rodenbacher Chaussee 4, 63457 Hanau, Germany*

E-mail: shivangi.singh@chalmers.se; ghj@chalmers.se

Quantification of Brønsted acid sites during NH_3-TPD

To quantify the Brønsted acid sites, the 100 h hydrothermally aged catalyst was used as a baseline, under the assumption that this sample has lost all the Brønsted acid sites. This reference is subtracted from NH_3-TPD signal for each sample as shown in Figure S1. To estimate the amount of Brønsted acid sites, the curve are integrated using trapezoid rule.

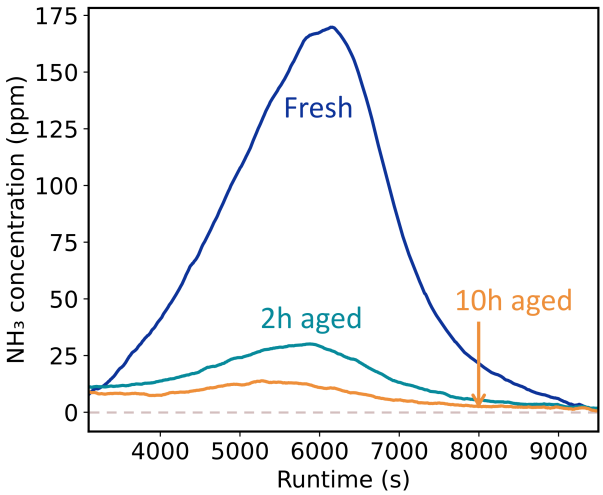

Figure S1: 100 h baseline corrected NH_3-TPD for fresh, 2 h and 10 h aged samples.

The amount of Brønsted acid sites was also estimated by Gaussian peak fitting. The results for the two methods are compared in Table 1 for the fresh sample and the the samples aged 2 and 10 hours. The Brønsted acid sites decreased quickly during the first 2 hours of hydrothermal aging, followed by a much slower loss at longer aging times. The same trend was observed from both the methods.

Table S1: Gaussian fitting results compared with 100 h baseline data for different samples.

Sample	**Gaussian fitting**	**100 h baseline**
Fresh	1353	1229
2 h aged	357	265
10 h aged	280	129

Degree of Rate Control Analysis for NH_3-SCR

A degree of rate control (DRC) analysis[S1,S2] was performed to identify the elementary steps that control the overall reaction rate. The DRC for each elementary step i is defined as:

$$X_i = \frac{\partial \ln r}{\partial \ln k_i}, \tag{1}$$

where r is the reaction rate for N_2 formation and k_i is the rate constant of elementary step i. The sensitivity was evaluated numerically using a central finite-difference scheme. Each elementary step was perturbed by $\pm 1\%$, i.e., $k_i \rightarrow k_i(1 \pm \varepsilon)$ with $\varepsilon = 0.01$. The DRC was then calculated as:

$$X_i \approx \frac{\ln r^+ - \ln r^-}{\ln(1+\varepsilon) - \ln(1-\varepsilon)}, \tag{2}$$

where r^+ and r^- denote the reaction rates obtained from the positively and negatively perturbed rate constants, respectively.

HONO and H_2NNO decomposition over Brønsted acid sites

At low temperatures, the rate of the NH_3–SCR reaction is mainly determined by the NO adsorption step on *-OO-*, which arises from the strong inhibitory effect of adsorbed NH_3, which blocks the the Cu-sites. As the temperature increases toward 200 °C, the controlling influence of NO adsorption gradually diminishes, whereas the formation of NO on *-HOOH-* becomes increasingly important. Furthermore, the N_2O formation acts as a competing pathway and has a negative degree of rate control. All the rate controlling steps takes are connected to the Cu-sites when the HONO and H_2NNO decomposition takes place over Brønsted acid sites.

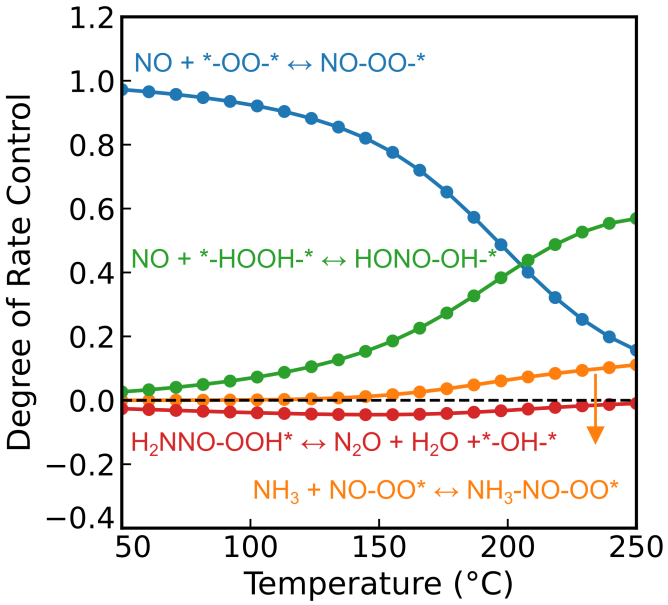

Figure S2: Degree of rate control analysis for NH_3-SCR over Cu-CHA when HONO and H_2NNO are decomposed over Brønsted acid sites. The simulation is performed with 600 ppm NH_3, 500 ppm NO, 10% O_2, and 5% H_2O balance N_2.

HONO and H_2NNO decomposition over silanols

At low temperatures, the rate of the NH_3–SCR reaction is mainly determined by the NO adsorption step on *-OO-*. As the temperature increases toward 150 °C, the controlling influence of NO adsorption gradually diminishes, whereas the formation of NO on *-HOOH-* and H_2NNO decomposition to N_2 and H_2O over silanols becomes increasingly important, particularly at intermediate temperatures. In this case, the rate controlling steps are both over Cu sites and silanol nests.

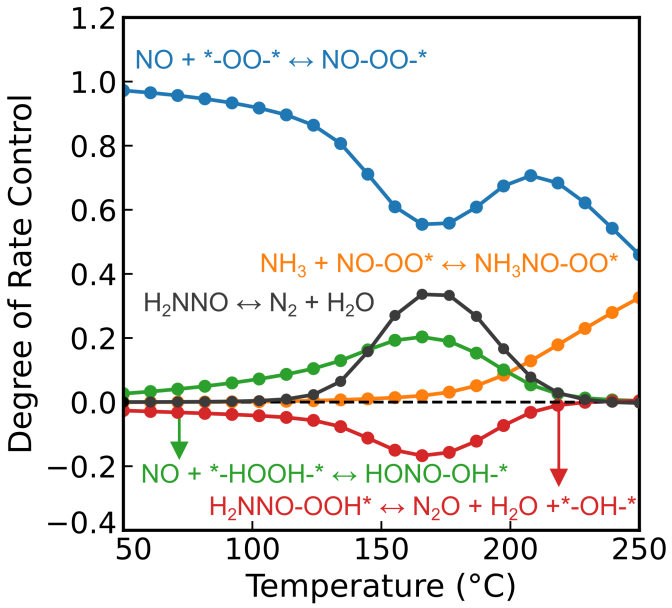

Figure S3: Degree of rate control analysis for NH_3-SCR over Cu-CHA when HONO and H_2NNO decomposition takes place over silanol nests. The simulation is performed with 600 ppm NH_3, 500 ppm NO, 10% O_2, and 5% H_2O balance N_2.

Kinetic parameters used in the simulations

Table S2 reports the kinetic parameters used in the simulations. The values are taken from Ref.[S3] except r17 to r19, which are evaluated in the present work. The turn over frequency is calculated as the number of consumed NO per Cu-complex accounting for the probability of having two Cu-complexes in the same CHA cage. The probability of having two $[Cu(NH_3)_2]^+$ complexes in the same cage is determined by the relative stability of paired and separated complexes. The relative stability depends on the aluminum distribution together with how far the complexes are from the original Al-site. Based on our previous work,[S3] we put the probability of having two complexes in the same cage to be $6{\times}10^{-4}$.

Table S2: Energy ($\Delta E^{\ddagger}$) and entropy ($\Delta S^{\ddagger}$) contributions to the reaction barriers of the considered elementary steps. Reaction r20 involves the separation of the paired linear complexes, resulting in the stoichiometric 2 on the product side. Energy is given in eV and entropy is J/mol $\cdot$ K. The $*$ in the elementary steps represents one $[Cu(NH_3)_2]^+$ complex.

no.	**elementary step**	$\Delta \boldsymbol{E}_f^{\ddagger}$	$\Delta \boldsymbol{E}_b^{\ddagger}$	$\Delta \boldsymbol{S}_f^{\ddagger}$	$\Delta \boldsymbol{S}_b^{\ddagger}$
	$O_2 + 2* \xleftrightarrow{r_1} *\text{-OO-}*$	0.13	0.33	-134.9	17.6
r1	$O_2 + 2* \xleftrightarrow{r_1} *\text{-OO-}*$ (ΔE & ΔS from Exp.)	0.13	0.95	-104.9	17.6
r2	$NO + *\text{-OO-}* \xleftrightarrow{r_2} \text{NO-OO-}*$	0.00	0.70	-109.2	0.0
r3	$NH_3 + \text{NO-OO-}* \xleftrightarrow{r_3} NH_3\text{NO-OO-}*$	0.00	0.31	-65.6	0.0
r4	$NH_3\text{NO-OO-}* \xleftrightarrow{r_4} H_2\text{NNO-OOH-}*$	0.05	0.54	-2.5	-44.4
r5	$H_2\text{NNO-OOH-} * + S \xleftrightarrow{r_5} H_2\text{NNO-S} + *\text{-OHO-}*$	0.30	0.60	0.0	0.0
r6	$NO + NH_3 + *\text{-OHO-}* \xleftrightarrow{r_6} H_2\text{NNO-OH-OH}$	0.16	0.60	-3.2	38.8
r7	$H_2\text{NNO-OH-OH} + S \xleftrightarrow{r_7} H_2\text{NNO-S} + *\text{-OHOH-}*$	0.30	0.60	0.0	0.0
r8	$NO + *\text{-OHOH-}* \xleftrightarrow{r_8} \text{HONO-OH-}*$	0.10	0.39	-120.9	0.0
r9	$\text{HONO-OH-} * + S \xleftrightarrow{r_9} \text{HONO-S} + *\text{-OH-}*$	0.30	0.60	0.0	0.0
r10	$NO + *\text{-OH-}* \xleftrightarrow{r_{10}} [\text{HONO-} * + *]$	0.10	1.03	-120.9	0.0
r11	$[\text{HONO-} * + *] + S \xleftrightarrow{r_{11}} \text{HONO-S} + 2*$	0.30	0.60	0.0	0.0
r12	$NH_3 + *\text{-OH-}* \xleftrightarrow{r_{12}} [NH_3\text{-OH-} * + *]$	0.00	0.97	-90.4	0.0
r13	$NO + [NH_3\text{-OH-} * + *] \xleftrightarrow{r_{13}} [\text{HONO-}NH_3\text{-} * + *]$	0.00	0.32	-120.9	0.0
r14	$[\text{HONO-}NH_3\text{-} * + *] + S \xleftrightarrow{r_{14}} NH_3 + \text{HONO-S} + 2*$	0.30	0.60	90.4	0.0
r15	$NH_3 + *\text{-OO-}* \xleftrightarrow{r_{15}} NH_3\text{-OO-}*$	0.00	0.98	-103.8	0.0
r16	$H_2\text{NNO-OOH-}* \xleftrightarrow{r_{16}} N_2O + H_2O + *\text{-OH-}*$	0.40	2.61	2.7	-301.4
r17	$H_2O + *\text{-OO-}* \xleftrightarrow{r_{17}} H_2O\text{-OO-}*$	0.00	0.79	-124.91	0.0
r18	$H_2O + *\text{-OHOH-}* \xleftrightarrow{r_{18}} H_2O\text{-OHOH-}*$	0.00	0.66	-110.66	0.0
r19	$NH_3 + *\text{-OHOH-}* \xleftrightarrow{r_{19}} NH_3\text{-OHOH-}*$	0.00	0.75	-103.8	0.0
	On Brønsted acid sites				
r20	$NH_3 + \text{HONO-S} \xleftrightarrow{r_{27}} H_2\text{NNO-S} + H_2O$	0.38	0.93	19.7	-194.6
r21	$H_2\text{NNO-S} \xleftrightarrow{r_{28}} H_2O + N_2 + S$	0.38	2.08	-70.1	-294.4
	On Silanol nest				
r20	$NH_3 + \text{HONO-S} \xleftrightarrow{r_{27}} H_2\text{NNO-S} + H_2O$	0.42	1.03	19.7	-194.6
r21	$H_2\text{NNO-S} \xleftrightarrow{r_{28}} H_2O + N_2 + S$	0.59	3.21	-70.1	-294.4

References

(S1) Campbell, C. T. Future Directions and Industrial Perspectives Micro- and Macro-Kinetics: Their Relationship in Heterogeneous Catalysis. *Top. Catal.* **1994**, *1*, 353–366.

(S2) Campbell, C. T. The degree of rate control: A powerful tool for catalysis research. *ACS Catal.* **2017**, *7*, 2770–2779.

(S3) Feng, Y.; Wang, X.; Janssens, T. V. W.; Vennestrøm, P. N. R.; Jansson, J.; Skoglundh, M.; Grönbeck, H. First-Principles Microkinetic Model for Low-Temperature NH_3-Assisted Selective Catalytic Reduction of NO over Cu-CHA. *ACS Catal.* **2021**, *11*, 14395–14407.